

A comparative assessment of the seismic response of an earthen dam using analytical simulation and empirical methods

Srijit Bandyopadhyay¹, Raj Banerjee¹, Aniruddha Sengupta^{2,*}, Y. M. Parulekar¹ and G. R. Reddy³

¹Bhabha Atomic Research Centre, Trombay, Mumbai 400 085, India

²Civil Engineering Department, Indian Institute of Technology Kharagpur, Kharagpur 721 302, India

³Bhabha Atomic Research Centre, Trombay, Mumbai 400 085, India

This article presents the permanent deformation of an earthen dam located in the vicinity of a safety related structure for $M_w = 6.5$ design basis earthquake. A non-linear 2D dynamic analysis using a real earthquake motion compatible with the design spectrum was performed to check the earthquake-induced deformations of the dam. Deformations of the dam were also estimated by semi-empirical and empirical methods such as Seed and Makdisi's method, Newmark's double integration method, Jansen's method and Swaisgood's method. Results from different methods are compared to obtain a range for the value of permanent deformations of the dam. It is observed that the lateral deformation obtained by Seed and Makdisi's method is the highest while Jansen's method predicts the highest crest settlement. The crest settlement of the dam is found to vary between 11.8 mm and 17.8 mm, which is within the safety limits according to IITK-GSDMA guidelines.

Keywords: Earthen dam, dynamic analysis, deformations, non-linear finite element analysis.

THE main focus of this study is to predict the dynamic performance of Apsara dam using 2D plane strain finite element (FE) analysis. Apsara dam is 18.5 m high earthen embankment located in Trombay, a suburb of Mumbai in India. The area, being within 350 km from the Gulf of Cambay and Rann of Kutch, is known to be seismically active and has experienced several devastating earthquakes like Koyna (1967) and Bhuj (2001) in the near past. Also, Trombay region is located in the seismic Zone III (ref. 1) of India, a zone with moderate seismic hazard. Apsara dam was constructed in 1950. The seismic criteria used earlier for the design of nuclear research facilities were less rigorous than the present ones. For this reason, a new study was undertaken to check whether the dam satisfies the present seismic design criteria for

that region from the safety and serviceability point of view.

The determination of permanent deformation of a dam during a probable ground motion is one of the seismic safety criteria. However, estimation of permanent deformation of a dam due to seismic loadings is a complex task as it involves many factors and lacks reliable field data during an earthquake. A ground motion is unique to a site for a particular earthquake. When real earthquake data is not available, the site-specific spectral compatible time history is used. The response of a dam is affected by the type of construction, water level in the reservoir, height of the dam, etc.². Nowadays sophisticated numerical tools like finite element method, finite difference method are available for assessing the dynamic response of a dam. But a realistic deformation value of a dam obtained from these advanced numerical tools may be expected only when the material parameters and numerical models accurately represent the actual conditions existing at a site. Despite several limitations, an advanced numerical analysis is recommended for performing the earthquake safety evaluation of a dam. Over the decades, starting with the fifth Rankine lecture by Newmark³, several simplified empirical, semi-empirical methods³⁻⁶ have been proposed to evaluate the permanent deformation of a dam during an earthquake. Due to limited availability of such studies, all the empirical and semi-empirical relations are developed based on the statistical analysis of these limited data.

Singh *et al.*⁷ conducted finite element analyses of several earthen dams affected by the 2001 Bhuj ($M_w = 7.6$) earthquake which were within 50 km of the epicentre. These dams underwent free-field ground motions with peak ground accelerations (PGAs) between 0.28 and 0.52 g. Basudhar *et al.*⁸ conducted 2D finite element (FEM) seismic analyses of Tehri dam located in a seismically active region for studying displacement, velocity and acceleration time histories near the crest and bottom of the dam using the acceleration time history of 2001 Bhuj earthquake. Their results revealed that vertical

*For correspondence. (e-mail: sengupta@civil.iitkgp.ernet.in)

displacement at any location of an embankment dam was negligibly small compared to horizontal displacement. The velocity time history shows a maximum velocity in forward direction at the crest of the dam, while in the reverse direction, the same is experienced by shell and core of the dam supplemented by a noticeable phase difference. The accelerations obtained near the crest of a dam will be more than those near its bottom portions.

The present article provides an estimate of the permanent deformations of Apsara embankment dam subjected to an earthquake of magnitude, $M_w = 6.5$ and a PGA of 0.156 g by a plane strain finite element method and compares them with those obtained by some of the well-established semi-empirical and empirical methods.

Description of the dam

Apsara dam is an earthen zoned dam. It has a maximum height of 18.5 m at the deepest location. The crest has a width of 2 m and spans 500 m in length. The foundation of the dam lies on top of a weathered rock of thickness 10 m overlying a solid rock base. The dam consists of a central impervious core consisting of compacted clay with a width of 18 m at the base and tapers to a width of 1.5 m just one metre below the crest. A 900 mm thick filter/drain layer is located on the downstream side of the core. The central clay zone is protected by rockfills on both downstream and upstream sides. The downstream slope is 1(V):2(H) and the upstream slope is 1(V):2.5(H). The upstream slope is provided with stone revetment to protect against surface erosion. A cut-off trench is also provided underneath the clay core along the length of the dam for seepage control. A free draining rockfill toe is provided on the downstream for additional stability. A freeboard of 2 m is provided at the crest of the dam. The storage capacity of the reservoir is around 120 million litres. At one end of the dam, a surplus weir of 12.2 m in length and 2.2 m in width is provided to let the surplus water overflow onto the downstream side. Figure 1 a shows a typical section of the dam.

Material properties

The shear strengths of the dam materials are obtained from *in situ* tests and laboratory triaxial tests and summarized in Table 1. In the present case, the following empirical relationship given by Seed and Idriss⁹ to find the shear modulus (G) of a cohesionless soil is utilized

$$G = 1000K(\sigma_0^{0.5}), \quad (1)$$

where G is in kPa, K is an empirical factor which is a function of the relative density of the soil (= 13.0 in this study) and σ_0 is the mean effective confining stress (in kPa).

For cohesive material, the shear modulus is obtained from the relationship given by Hardin and Drenvich¹⁰

$$G = \frac{3230(2.97 - e)^2}{(1 + e)} (\text{OCR})^k (\sigma_0)^{0.5}, \quad (2)$$

where G is in kPa, e the void ratio, σ_0 the mean effective confining stress (in kPa), OCR the over consolidation ratio, and k is a parameter which is a function of the plasticity index of the soil (=0.18 in this study).

The modulus of elasticity (E) of the soil is obtained from the equation

$$G = \frac{E}{2(1 + \gamma)}, \quad (3)$$

where γ is the Poisson's ratio of the soil.

Response spectrum and ground motion

The IS: 1893 (ref. 1) code gives the seismic zoning of India as per the comprehensive intensity scale of earthquakes (MSK64). Apsara dam is located in Zone III, a zone with moderate seismic hazard. The intensity associated with Zone III¹ is VII which corresponds to 0.156 g PGA and the corresponding local magnitude (M_L) is 5.67 based on the relationship proposed by Gutenberg and Richter¹¹. The corresponding moment magnitude (M_w) is around 5.9 proposed by Idriss¹². For the present study, an earthquake with M_w equal to 6.5 and the zero-period acceleration (PGA) to 0.156 g is selected. This value represents the maximum credible earthquake (MCE) for the region. The site-specific data or the uniform hazard response spectrum (UHRS) for this region is obtained from the probabilistic seismic hazard analysis (PSHA) study¹³ and shown in Figure 2 b. The above spectrum is considered as a representative ground motion for the finite

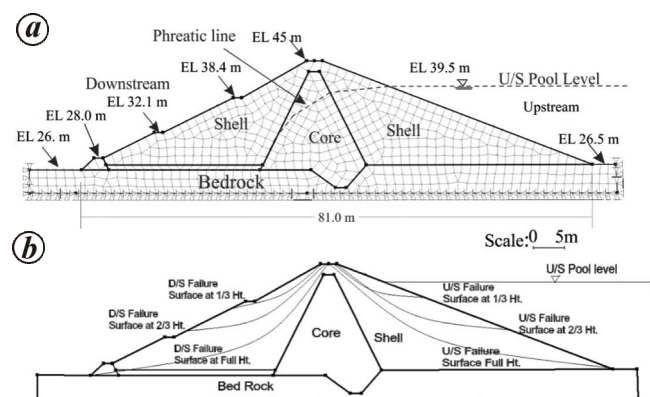


Figure 1. a, Typical cross-section and finite element discretization of Apsara dam; b, Locations of the upstream and downstream failure surfaces in a typical cross-section of Apsara dam.

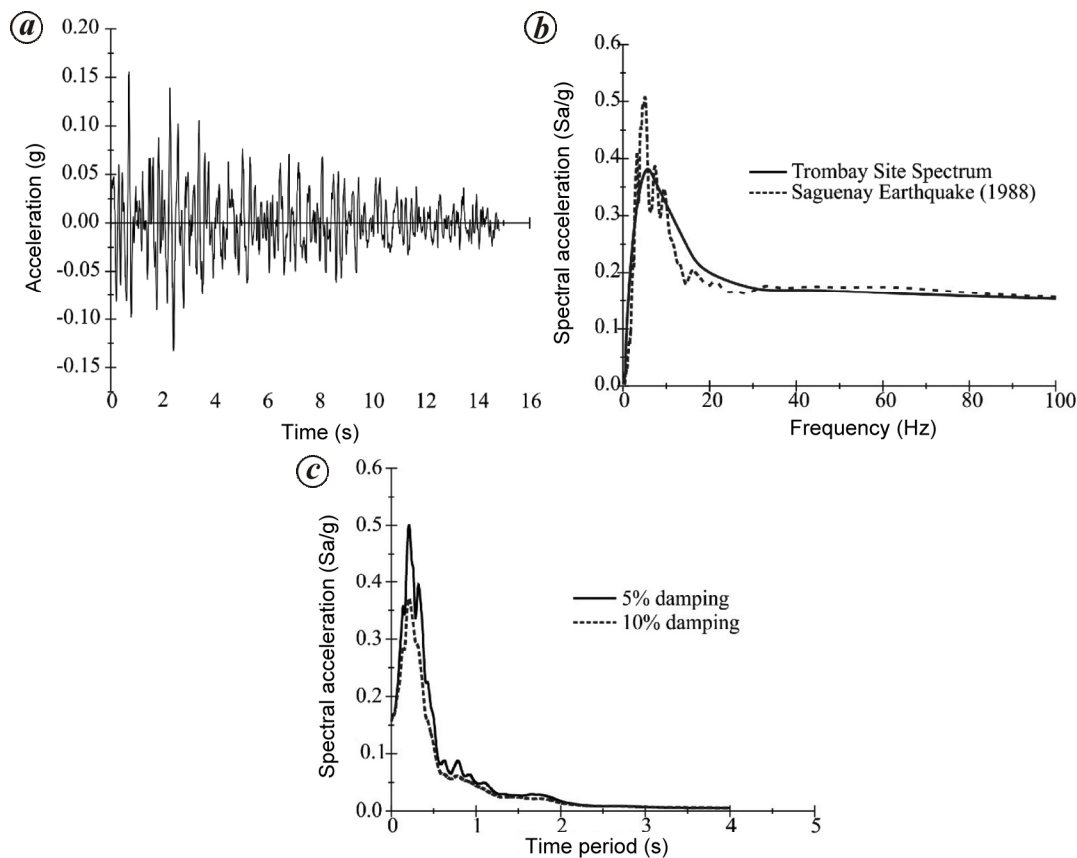


Figure 2. *a*, Selected ground motion used in 2D finite element analysis; *b*, Comparison of Trombay response spectra and that of Saguenay earthquake (Canada), 1988; *c*, Response spectra of Saguenay Earthquake (Canada), 1988 at 5% and 10% of critical damping.

Table 1. Material strength parameters

Soil properties	Zones of dam		
	Clay core	Shell (U/S and D/S)	Coarse filter
Bulk unit weight (kN/m ³)	19.2	21	20
Saturated unit weight (kN/m ³)	19.5	22	20
Angle of internal friction	15°	37°	42°
Cohesion (kPa)	30	0	0

element analysis of Apsara dam. A number of real earthquakes are reviewed and the Saguenay Earthquake of Canada (25 November 1988), Site 7 ($M_w = 6.5$, NW component) (see Figure 2a) was chosen based on its PGA and frequency content of the motion. The selected motion is a bed rock motion with a focal depth of 29 km, an epicentre distance of 45.14 km with a predominant frequency of 4 Hz. The ground motion was chosen such that its frequency content matches with the predominant time period of the dam, which typically lies between 0.1 sec and 1 sec (ref. 14). The selected earthquake motion has a predominant time period, PGA, velocity and displacement of 0.34 sec, 153.036 cm/s², 8.402 cm/s and 56 cm

respectively. The ratio of the maximum velocity and acceleration (v_{max}/a_{max}) is 0.054, which is less than 0.1, confirms that it is a rock motion³. Figure 2b compares the site-specific response spectra (at 5% damping) and spectra of the selected ground motion. A good match is observed between the response spectra of selected motion and the site-specific spectra which confirms the adequacy of the selected ground motion.

Methodology

Analysis using equivalent linear approach

The ‘shear beam’ concept serves as a basis for many of the recently developed models. To obtain the natural frequencies and mode shapes of the dam, the response spectrum is analysed in which the dam is modelled as a triangular shear beam with variable stiffness. The response spectra at 5% and 10% of critical damping used in the shear beam analysis for $M_w = 6.5$, PGA = 0.156 g earthquake are shown in Figure 2c. The dependence of soil modulus on the confining pressure has been established by Ghaboussi and Wilson¹⁵. Using the well-established distributions of static confining stresses in an

idealized dam section, along with the assumption that the element soil modulus, $G(z)$, increases in proportion to $\sigma_0^{0.5}$, many researchers recommended the following dimensionless expression to be used to estimate $G(z)$ with the depth with a reasonable accuracy^{9,10,16}

$$G = G_b \left(\frac{z}{H} \right)^m, \quad (4)$$

where m is the material non-homogeneity parameter, G_b the shear modulus at the base of the dam, z the depth from crest of the dam and H is the total height of the dam.

Based on the above expressions, an inhomogeneous shear beam analysis is conducted for clay core of the dam by using the principle of an equivalent linear approach in which the strain-dependent dynamic soil properties are estimated in an iterative process for a certain value of material non-homogeneity parameter, m ($= 0.5$ in this study). The curves proposed earlier^{9,17} are used to represent the strain-dependent dynamic stiffness and damping of the clayey material as shown in Figure 3. The results of the shear beam analysis in terms of maximum crest acceleration, fundamental period of the dam, damping ratio and the corresponding shear strain are shown in Table 2.

Table 2. Results of the shear beam analysis

Magnitude of earthquake, $M_w = 6.5$	
Maximum crest acceleration, a_{\max}	0.50 g
Average equivalent strain	0.033%
Strain compatible damping	6.5%
Fundamental time period	0.218 sec
2nd mode time period	0.105 sec
3rd mode time period	0.069 sec

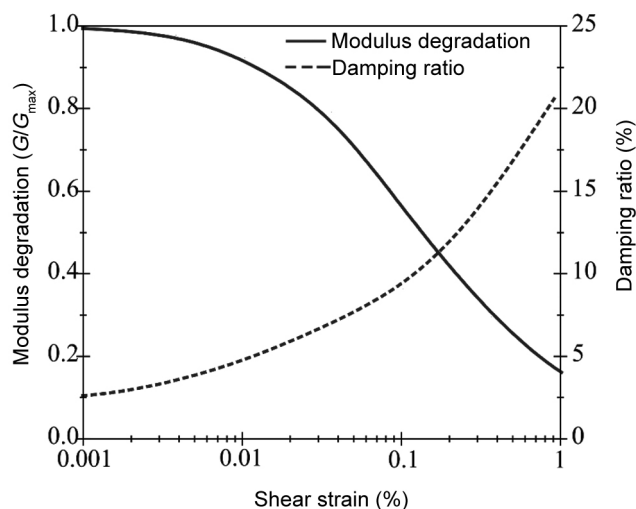


Figure 3. Dependency of soil stiffness and damping of clay core on strain level.

Nonlinear dynamic analysis

The finite element discretization of Apsara dam is shown in Figure 1a. The embankment dam and its foundation are modelled by 4-noded and 3-noded 2D plane strain finite elements. The finite element mesh consists of 639 nodes and 597 elements. The material properties of each zone are specified in Table 1. For static analysis, a fixed boundary condition is applied at the bottom, which restricts the movements in both horizontal and vertical directions, whereas the two sides are restricted to move in the horizontal direction. In dynamic analysis, an absorbing boundary is applied at the two side boundaries to minimize the reflection of waves. Finite element analysis is performed in three stages – in the 1st stage, the entire problem is solved in the presence of gravity (or self-weight) only. In the present study, the construction sequence of the dam is ignored. In the next stage, a steady state analysis is performed where the reservoir is impounded. The seismic response of the dam at normal operating condition is then analysed using acceleration time history of the selected Saguenay earthquake (1988) of PGA 0.156 g. The selected ground motion is shown in Figure 2a. The motion is applied at the bottom of the foundation for 15 sec. Deformation of the dam and change in the pore water pressures due to earthquake motions are obtained from the analysis.

Figure 4 shows the deformed geometry of the dam at the end of the dynamic analysis. The predominant deformations of the dam are found to be in its downstream shell. Vertical settlement is obtained near the dam's crest and the lateral deformation obtained at the upstream face as shown in Figure 5a and b. The pore water pressure variation near the bottom and mid-point of the dam's core is shown in Figure 6. The analysis predicts no liquefaction for the dam and its foundation for this earthquake event. The response of the input acceleration is measured at the top of the dam. Figure 7 shows the amplification of motion at the dam's crest and accordingly, the amplification of PGA is around 2.21 times at the crest. However, different amplification value of 3.2 times the base motion is obtained in the shear beam analysis of the dam. A possible reason for this deviation is due to the onset of non-linear (damping) behaviour of the dam materials during earthquake motions, which prevents the development of high acceleration predicted by shear beam analysis¹⁶.

Besides the shear beam and FEM analysis, several empirical and semi-empirical methods exist to estimate the permanent displacement in an earthen embankment during an earthquake.

Estimation of lateral displacements of a dam by Seed and Makdisi

This is a simple yet rational approach to the design of an embankment dam under earthquake loadings. The method

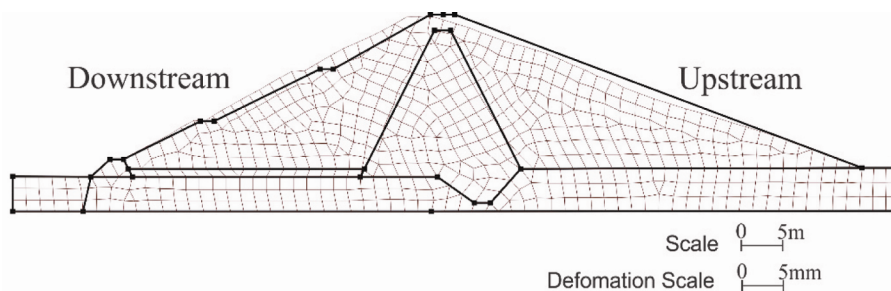


Figure 4. Deformed geometry of the dam at the end of the earthquake (deformation magnified 1000 times).

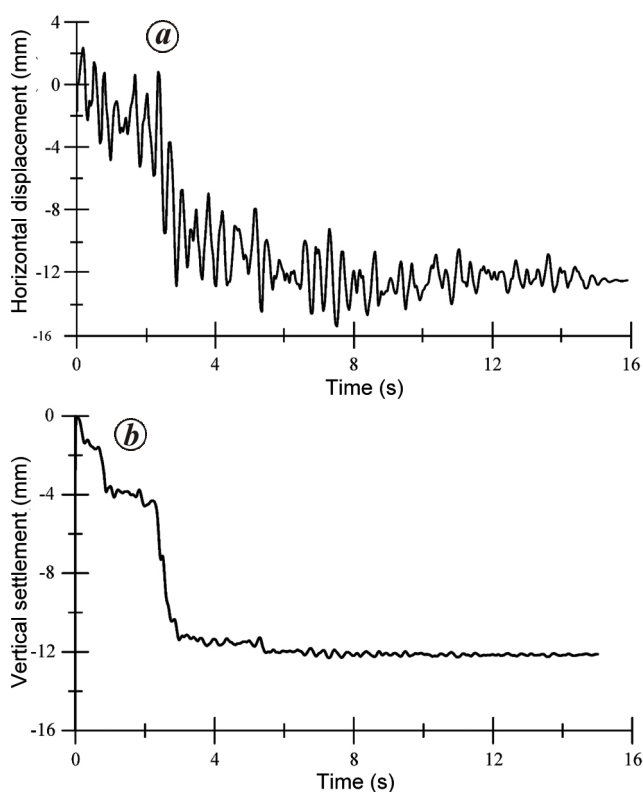


Figure 5. a, Lateral deformation at the upstream berm of the dam; b, vertical settlement at the crest of the dam.

is based on the concept that whenever the rigid body acceleration, K_{max} for a sliding area exceeds the yield acceleration, K_y , a permanent deformation takes place. The yield acceleration is determined from a series of pseudostatic analyses. After obtaining the yield acceleration, the permanent deformation U is calculated, which is a function of an earthquake magnitude and fundamental period of a dam for a given ratio of K_y/K_{max} .

The yield acceleration K_y is defined as an acceleration at which a potential sliding surface would develop a factor of safety of unity. Yield accelerations are obtained for three failure masses on the upstream and downstream faces of the dam whose locations are shown in Figure 1 b. The water level on the upstream face is assumed to be at E l.16 m (maximum normal operating pool) and the factor

of safety is determined according to Bishop's simplified method¹⁸. The results of the factor of safety and the corresponding values of yield acceleration, K_y , are summarized in Table 3.

Considering the approximate nature of the method, the average relationship⁴ adopted for determining the maximum average acceleration for a potential sliding mass based on the maximum crest acceleration, is considered accurate enough for practical purposes. For design purposes, a conservative estimate of the accelerations is desirable. Hence, the upper limit curve is used in the present study. The maximum average acceleration along with the K_y/K_{max} values for all cases is illustrated in Table 4 and the lateral permanent displacements U , for each of the failure surface is calculated from the figure given in Makdisi and Seed⁴. The corresponding displacements thus obtained for $M_w = 6.5$ earthquake are shown in Table 5.

This approach has two drawbacks; the peak acceleration at the crest (k_{max}) is highly variable, and the frequency content of the motion is not captured in shear beam analysis. In addition, the range of the upper and lower bounds on the Makdisi and Seed⁴ plot of k_{max}/PGA versus y/h and k_y/k_{max} versus displacement (U) may not be true, because of the limited number of analysis of the earth structure with variable ground motion. These curves need refinement and upgradation as a larger number of analytical results for embankments are obtained.

Estimation of displacements of a dam by Newmark's method

Newmark³ proposed a method of computing a seismically induced deformation based on the sliding wedge concept. When the inertia of the mass exceeds the frictional resistance along the sliding surface, the sliding failure of the mass occurs and the corresponding relative displacements are calculated by double integration of the difference between mass acceleration and the yield acceleration K_y .

A concept of 'elastic response method' has been proposed by Seed and Martin¹⁹ to determine the amplified absolute acceleration time history at any point in the dam.

Table 3. Yield accelerations

Zones of dam	Location of surface	FS in static case	Yield acceleration (K_y)	K_{max} (g)	K_y/K_{max}
Upstream slope	1/3 height	2.207	0.28	0.455	0.615
	2/3 height	2.101	0.20	0.310	0.645
	Full height	2.051	0.19	0.250	0.760
Downstream Slope	1/3 height	1.444	0.13	0.455	0.28
	2/3 height	1.628	0.215	0.310	0.69
	Full height	1.733	0.25	0.250	1.00

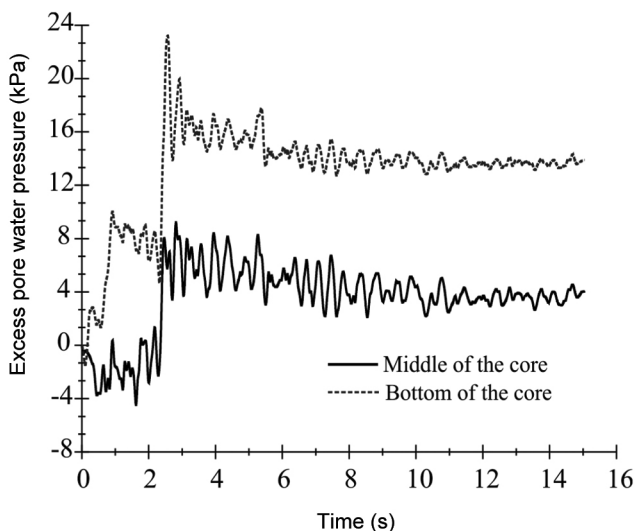


Figure 6. Variation of pore water pressure near the bottom and mid-point of the core of the dam.

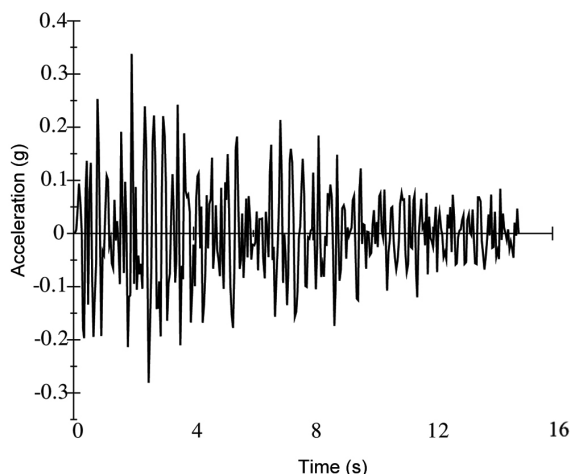


Figure 7. Acceleration time history at the crest of the dam.

According to this concept, damped response to the random ground motion, u_g , which might be induced by an earthquake, can be shown by

$$u(y,t) = \sum_{n=1}^{\infty} \frac{2J_0\left(\beta_n \frac{y}{H}\right)}{\omega_{dn}\beta_n J_0(\beta_n)} \int_0^t \ddot{u}_g e^{-D_n \omega_n(t-\tau)} \sin(\omega_{dn}(t-\tau)) d\tau \tag{5}$$

The total or absolute acceleration, \ddot{u}_g acting on the dam at any time t , is given by

$$\ddot{u}_a(y,t) = \ddot{u}(y,t) + \ddot{u}_g(t). \tag{6}$$

where y is the depth from the crest of the dam, u_g the base acceleration and u_a is the total acceleration.

This may be readily determined from the values of $u(y,t)$ and the known values of ground acceleration. Hence, the absolute acceleration y , at any level, in the dam at t , is expressed by

$$\ddot{u}_a(y,t) = \sum_{n=1}^{\infty} 2\omega_n \frac{1}{\beta_n J_1(\beta_n)} J_0\left(\beta_n \frac{y}{H}\right) \times \int_0^t \ddot{u}_g e^{-\lambda_n \omega_n(t-\tau)} \sin(\omega_n(t-\tau)) d\tau, \tag{7}$$

where n is the number of significant mode shapes to be considered in the analysis. In the present analysis, three mode shapes are considered. The above equation is solved for 1/3rd, 2/3rd and full heights of the dam.

The actual irregular acceleration time history is converted into equivalent time history of several cycles of constant amplitude as proposed by Seed and Idriss²⁰. The present time history is modelled by six cycles of identical full sinusoidal waves of average acceleration amplitude, a_{avg} ($=2/3$ of PGA) of 0.30, 0.21 and 0.104 g for the upper 1/3rd, 2/3rd and full height of the dam respectively.

The acceleration time history is represented by an equivalent sine wave given by

$$K(t) = a_{avg} \sin\left(2\pi \frac{t}{T}\right), \tag{8}$$

where T is the fundamental period of the dam ($= 0.218$ sec in the present case).

Based on the procedure by Sengupta¹⁴, the relative displacements of the dam at 1/3rd height are found to be 2 mm for the upstream side and 76 mm for the downstream side. No significant deformations are observed at 2/3rd and full height of the dam from the above methodology.

Table 4. Permanent displacements by Makdisi and Seed's procedure

Location of sliding surface	Depth y/H	Upstream			Downstream		
		K_y/K_{max}	$U/K_{max}gT_0$	U (mm)	K_y/K_{max}	$U/K_{max}gT_0$	U (mm)
1/3 height	0.33	0.615	0.0085	8.27	0.28	0.08	77.84
2/3 height	0.66	0.645	0.006	3.97	0.69	0.0058	3.845
Full height	1.00	0.760	0.004	2.14	1.00	–	–

Table 5. Comparison of deformations (lateral and vertical)

Methods used	Deformations (mm) due to the $M_w = 6.5$ earthquake	
	Lateral displacement (mm)	
	Upstream	Downstream
Seed and Makdisi's	8.27	77.84
Double integration	2.0	76.0
2D finite element method	13.69	9.05
Crest settlement (mm)		
Jansen's	17.80	
Swaisgood's	11.80	
2D finite element method	12.32	

One of the basic assumptions to calculate seismic displacement according to this method is that the failure mass is considered to be totally rigid. This means that the dynamic response of the slope and embankment, for which the seismic stability is estimated, is not considered calculating seismic displacement. The soil slopes and embankments are flexible systems characterized by a relatively large fundamental period. In order to consider this for the estimation of seismic displacement of a slope, a decoupled method is proposed by Makdisi and Seed⁴ which consists of two steps. The first step focusses on the estimation of dynamic response of the failing soil mass in terms of an equivalent acceleration time history after calculation of response of the earth structure. The time history of an equivalent horizontal acceleration is defined as the integral of horizontal stresses respectively, along the slip surface divided by the weight of the sliding mass. In the second step, the permanent seismic displacement is obtained from double integration of the relative acceleration. Difference between the applied and critical acceleration is defined as the relative acceleration. A decoupled sliding block analysis overestimates the system's response, because the forces at the sliding interface are not taken into account, when considering the dynamic response.

A decoupled sliding block analysis does not correctly model the forces at the sliding interface, which leads to an over-prediction of the system response.

Crest settlement is considered for an earthquake related damage and deformation, because it is often the most quantified measurement of damage in such cases. This parameter also has a relationship with the severity of deformations and cracking in a dam during an earthquake.

Estimation of crest settlement by Jansen's method

Jansen's⁵ method for estimating the crest settlement of a dam is based on the data collected from one hypothetical and four existing dams. A relationship is developed for computing crest settlement based on earthquake magnitude, maximum crest acceleration, K_m and yield acceleration, K_y , as follows

$$U(\text{cm}) = \left\{ 48.26 \left(\frac{M_w}{10} \right)^8 \frac{(K_m - K_y)}{\sqrt{K_y}} \right\}. \tag{9}$$

The value of crest amplification of Apsara dam is obtained from Jansen's method⁵. The corresponding crest settlement, U , at different locations is shown in Table 6. From the tabulated values, it may be concluded that the maximum range of crest settlement of Apsara dam lies between 12.6 and 17.8 mm respectively, for a $M_w = 6.5$ earthquake.

The above equation implies no deformation if maximum crest acceleration $K_m \leq K_y$ and it also calculates crest settlement without considering the height of the dam.

Estimation of crest settlement by Swaisgood's method

Swaisgood⁶ developed a crest settlement relationship based on 69 case histories which takes into account the level of severity of deformation and cracking in the dam.

Table 6. Estimation of crest settlement by Jansen's method

Value of K_m (g)	M_w	Location of sliding surface	Upstream slope		Downstream slope	
			K_y (g)	U (cms)	K_y (g)	U (cms)
0.546	6.5	1/3 height	0.28	0.77	0.13	1.78
		2/3 height	0.20	1.19	0.215	1.09
		Full height	0.19	1.26	0.25	0.92

Here, the crest settlement depends on the earthquake magnitude and PGA at the site as given below

$$\Delta(\%) = SEF \cdot K_{typ} \cdot K_{dh} \cdot K_{at}, \quad (10)$$

where $\Delta(\%)$ is the crest settlement (in percentage) of the dam and the alluvial thickness, SEF the site energy factor related to the earthquake magnitude (M) and PGA, and expressed as $SEF = e^{(0.7168M + 6.405PGA - 9.098)}$, K_{typ} a constant related to the type of dam construction (=1.363 for earthfill dam), K_{dh} a constant related to the dam height and expressed as $K_{dh} = 9.134 \cdot DH^{-0.437}$ where DH is the height of the dam in feet. K_{at} a constant related to the alluvial thickness and expressed as $K_{at} = 0.851 \cdot e^{(0.00368 \cdot At)}$ where At is the alluvial thickness in feet.

The estimated crest settlement of the dam for the seismic energy and site-specific factors recommended by Swaisgood is found out to be 11.80 mm.

In Swaisgood method, the accuracy for predicting crest settlement depends on the accuracy with which the site-specific PGA is estimated from probabilistic studies. In addition, crest deformation of the dam mainly spreads and settles during an earthquake event. There is no distinct failure along a particular shear plane.

Results and discussion

A comparison of displacements (both horizontal and vertical) of Apsara dam predicted by various methods is shown in Table 5. The results indicate a wide variation in values obtained from different methods. This may be due to the fact that these empirical and semi-empirical methods have very little in common. For a $M_w = 6.5$ earthquake, the lateral displacements of the upstream and downstream shells are in the range of 2–13.69 mm and 9.05–77.84 mm respectively. The crest settlement obtained from empirical methods varies between 11.8 and 17.8 mm. From the 2D plane strain finite element analysis, lateral displacement is found to be around 12.32 mm which is in reasonable agreement with values obtained from analytical procedures. As per IITK-GSDMA²¹ guidelines, the acceptable deformation of Apsara dam along any failure plane should not exceed 1 m. The range of deformations obtained by various methods lies well within this prescribed limit. Hence, it may be concluded

that lateral displacements and crest settlements of the dam during a probable earthquake are found to be within safety limits according to prescribed guidelines.

Conclusion

The variations in predicted displacements of Apsara dam under an earthquake motion indicate that there is still some room for understanding the failure mechanism of such a dam during a dynamic event. The finite element study shows that maximum deformation occurs on the upper portion of the dam, while the foundation level has negligible deformations. Among analytical methods, Makdisi and Seed method overestimates the deformations obtained, than those predicted by the double integration method and finite element analysis. From this study (refer to Table 5), it may be concluded that the evaluation of crest settlement by Swaisgood's method provide results closer to FEM results than Jansen's method.

1. USBR, Seismic design and analysis of embankment dams, Design Standards. Chapter 13, In *United States Department of the Interior, Bureau of Reclamation*, Denver, Colorado, DS-13(13)-7, 1989.
2. IS:1893, Indian Standard criteria for earthquake resistant design of structures, Part 1 – general provisions and buildings, Bureau of Indian Standards, Fifth Revision, New Delhi, 2001.
3. Newmark, N. M., Effects of earthquakes on dams and embankments. *Geotechnique*, 1965, **15**(2), 139–159.
4. Makdisi, F. I. and Seed, H. B., Simplified procedure for estimating dam and embankment earthquake induced deformations. *J. Geotech. Eng. Div.*, 1978, **104**(7), 849–867.
5. Jansen, R. B., Estimation of embankment dam settlement caused by earthquake. *Int. Water Power Dam Constr.*, 1990, **42**(12), 35–40.
6. Swaisgood, J. R., Estimating deformation of embankment dams caused by earthquakes. In ASDSO Western Regional Conference, Montana, USA, 1995, pp. 1–7.
7. Singh, R., Roy, D. and Jain, S. K., Analysis of earth dams affected by the 2001 Bhuj Earthquake. *Eng. Geol.*, 2005, **80**, 282–291.
8. Basudhar, P. K., Rao, N. S. V. K., Bhookya, M. and Dey, A., 2D FEM analysis of earth and rockfill dam under seismic condition. In 5th International Conference on Recent Advances in Geotechnical Earthquake Engineering and Soil Dynamics, 2010.
9. Seed, H. B. and Idriss, I. M., Soil modulus and damping factors for dynamic response analysis. Report EERC, 70–10, University of California, Berkeley, 1970.
10. Hardin, B. O. and Drenvich, V. P., Shear modulus and damping in soils: design equations and curves. *J. Soil Mech. Found. Div.*, 1972, **98**(7), 667–692.

RESEARCH ARTICLES

11. Gutenberg, B. and Richter, C. F., Earthquake magnitude, intensity, energy and acceleration (second paper). *Bull. Seismol. Soc. Am.*, 1956, **46**(2), 105–145.
12. Idriss, I. M., Evaluating seismic risk in engineering practice. In Proceedings of the 11th International Conference on Soil Mechanics and Foundation Engineering, San Francisco, USA, 1985, vol. 1, pp. 255–320.
13. Ghosh, A. K., Rao, K. S. and Kushwaha, H. S., Development for UHRS for Tarapur, Trombay and Kakrapara Sites. Report BARC/2003/E/019, 2003.
14. Sengupta, A., Estimation of permanent displacements of the Tehri dam in the Himalayas due to future strong earthquakes. *Sadhana*, 2010, **35**(3), 373–392.
15. Ghaboussi, J. and Wilson, E. L., Seismic analysis of earth dam reservoir systems. *J. Soil Mech. Found. Div.*, 1973, **99**(10), 849–862.
16. Dakoulas, P. and Gazetas, G., A class of inhomogeneous shear models for seismic response of dams and embankments. *Soil Dyn. Earthq. Eng.*, 1985, **4**(4), 166–182.
17. Seed, H. B. and Sun, J. H., Implication of site effects in the Mexico City earthquake of 19 September 1985 for Earthquake-resistance-design criteria in the San Francisco Bay Area of California. In Report No. UCB/EERC-89/03, University of California, Berkeley, USA, 1989.
18. Bishop, A. W., The use of slip circles in the stability analysis of earth slopes. *Geotechnique*, 1955, **5**(1), 7–17.
19. Seed, H. B. and Martin, G. R., The seismic coefficient in earth dam design. *J. Soil Mech. Found. Div.*, 1966, **92**(3), 25–58.
20. Seed, H. B. and Idriss, I. M., A simplified procedure for evaluating soil liquefaction potential. *J. Soil Mech. Found. Div., ASCE*, 1971, **97**(9), 1249–1274.
21. IIT-K, GSDMA guidelines for seismic design of earth dams and embankments, 2007.

Received 20 June 2016; revised accepted 9 March 2017

doi: 10.18520/cs/v113/i05/902-910
